Biochemical and Biophysical Research Communications 437 (2013) 585–590

Contents lists available at SciVerse ScienceDirect

Biochemical and Biophysical Research Communications

journal homepage: www.elsevier.com/locate/ybbrc

Structure of *N*-acetyl-L-glutamate synthase/kinase from *Maricaulis maris* with the allosteric inhibitor L-arginine bound

Gengxiang Zhao [a,b], Nantaporn Haskins [a,d], Zhongmin Jin [c], Norma M. Allewell [d], Mendel Tuchman [a,b], Dashuang Shi [a,b,*]

[a] Center for Genetic Medicine Research, Children's National Medical Center, Washington, DC 20010, USA
[b] Department of Integrative Systems Biology, The George Washington University, Washington, DC 20010, USA
[c] Southeast Regional Collaborative Access Team, Advanced Photon Source, Argonne National Laboratory, Argonne, IL 60439, USA
[d] Department of Cell Biology and Molecular Genetics and Department of Chemistry and Biochemistry, College of Computer, Mathematical, and Natural Sciences, University of Maryland, College Park, MD 20742, USA

ARTICLE INFO

Article history:
Received 28 June 2013
Available online 10 July 2013

Keywords:
N-acetyl-glutamate synthase
N-acetyl-glutamate kinase
GCN5-acetyltransferase
Arginine inhibition
Arginine biosynthesis
Allosteric regulation

ABSTRACT

Maricaulis maris *N*-acetylglutamate synthase/kinase (mmNAGS/K) catalyzes the first two steps in L-arginine biosynthesis and has a high degree of sequence and structural homology to human *N*-acetylglutamate synthase, a regulator of the urea cycle. The synthase activity of both mmNAGS/K and human NAGS are regulated by L-arginine, although L-arginine is an allosteric inhibitor of mmNAGS/K, but an activator of human NAGS. To investigate the mechanism of allosteric inhibition of mmNAGS/K by L-arginine, we have determined the structure of the mmNAGS/K complexed with L-arginine at 2.8 Å resolution. In contrast to the structure of mmNAGS/K in the absence of L-arginine where there are conformational differences between the four subunits in the asymmetric unit, all four subunits in the L-arginine liganded structure have very similar conformations. In this conformation, the AcCoA binding site in the *N*-acetyltransferase (NAT) domain is blocked by a loop from the amino acid kinase (AAK) domain, as a result of a domain rotation that occurs when L-arginine binds. This structural change provides an explanation for the allosteric inhibition of mmNAGS/K and related enzymes by L-arginine. The allosterically regulated mechanism for mmNAGS/K differs significantly from that for *Neisseria gonorrhoeae* NAGS (ngNAGS). To define the active site, several residues near the putative active site were mutated and their activities determined. These experiments identify roles for Lys356, Arg386, Asn391 and Tyr397 in the catalytic mechanism.

1. Introduction

A novel bifunctional enzyme that has both *N*-acetylglutamate synthase (NAGS, EC 2.3.1.1) and *N*-acetylglutamate kinase (NAGK, EC 2.7.2.8) activities and catalyzes the first two reactions in the L-arginine biosynthetic pathway was recently identified in some proteobacteria [1]. Interestingly, these bifunctional NAGS/K have higher protein sequence similarity to mammalian NAGS, a regulator of the urea cycle, than to the "classic" NAGS enzymes of most bacteria and plants. Bifunctional NAGS/K also exists in the same quaternary state and has a fold very similar to mammalian NAGS [2]. However, while both NAGS/K and mammalian NAGS are regulated by L-arginine, L-arginine is an allosteric inhibitor of NAGS/K but an allosteric activator of mammalian NAGS [3].

Structures of a "classic" NAGS from *Neisseria gonorrhoeae* (ngNAGS) with and without substrates and L-arginine bound indicate that this type of NAGS has a hexameric structure [4]. In contrast, *Maricaulis maris* NAGS/K, as well as NAGS/K from *Xanthomonas campestris* (xcNAGS/K), exists as tetramers [5]. Yeast NAGK (yNAGK) also forms tetramers, suggesting that tetrameric oligomerization is a common feature of non-classic NAGS and is evolutionarily conserved [6].

The catalytic and regulatory mechanisms of ngNAGS, are now well understood. However, no structures of a "non-classic" NAGS with L-arginine bound have been determined [5]. Although a

Abbreviations: AAK, amino acid kinase; GNAT, GCN5-related acetyltransferase; mmNAGS/K, *Maricaulis maris* *N*-acetyl-L-glutamate synthase/kinase; mmNAGS/K-Arg, mmNAGS/K bound with L-arginine; mmNAGS/K-CoA, mmNAGS/K bound with CoA; NAG, *N*-acetyl-L-glutamate; NAGK, *N*-acetyl-L-glutamate kinase; NAGS, *N*-acetyl-L-glutamate synthase; NAGS/K, *N*-acetyl-L-glutamate synthase/kinase; NAT, *N*-acetyltransferase; ngNAGS, *Neisseria gonorrhoeae* *N*-acetyl-L-glutamate synthase; RMSD, root mean standard deviation; tmNAGK, *Thermotoga maritima* *N*-acetyl-L-glutamate kinase; xcNAGS/K, *Xanthomonas campestris* *N*-acetyl-L-glutamate synthase/kinase; yNAGK, yeast *N*-acetyl-L-glutamate kinase.

* Corresponding author. Address: Center for Genetic Medicine Research and Department of Integrative Systems Biology, Children's National Medical Center, The George Washington University, 111 Michigan Avenue, N.W., Washington, DC 20010-2970, USA. Fax: +1 202 476 6014.
E-mail address: dshi@cnmcresearch.org (D. Shi).

0006-291X/$ - see front matter © 2013 Elsevier Inc. All rights reserved.
http://dx.doi.org/10.1016/j.bbrc.2013.07.003

mechanism for L-arginine regulation was proposed based on the structure of mmNAGS/K with CoA bound at a non-functional site, the L-arginine binding site and its regulatory mechanism have not been experimentally established.

Here, we report the structure of mmNAGS/K with L-arginine bound (mmNAGS/K-Arg) and compare it with the previously determined structure of mmNAGS/K with CoA bound, but without L-arginine bound (mmNAGS/K-CoA). Site directed mutagenesis was also used to probe the function of several amino acid residues at or near the active site. These structures and mutagenesis experiments provide experimental proof of the mechanism of L-arginine inhibition previously proposed [5].

2. Materials and methods

2.1. Protein expression and purification

mmNAGS/K, xcNAGS/K and all mutants were expressed and purified as described previously [7]. Briefly, the proteins were expressed in *Escherichia coli* BL21(DE3) cells (Invitrogen) and purified with nickel affinity and DEAE columns (GE Healthcare). Protein purity was verified by SDS/PAGE gel and protein concentration was measured with a Nano-drop 1000 spectrophotometer (Thermo Scientific). The extinction coefficient obtained from the ExPASy web server (http://web.expasy.org/protparam/) was used to calculate protein concentrations. The protein was stored at 253 K in a buffer containing 50 mM Tris–HCl, pH 8.0, 50 mM NaCl, 10% glycerol, 5 mM β-mercaptoethanol and 1 mM EDTA.

2.2. Site-directed mutagenesis

Site-directed mutant genes of mmNAGS/K and xcNAGS/K were created using primers containing the desired mutations and the QuikChange Mutagenesis Kit according to the manufacturer's protocol (Strategene). The sequences of mutant DNA sequences were verified by DNA sequencing.

2.3. Activity assay

Enzymatic activity was determined by measuring *N*-acetyl-L-glutamate (NAG) production as described previously using stable isotope dilution and liquid chromatography mass spectrometry (LC–MS) [8]. The assay was performed in a solution containing 50 mM Tris, pH 8.5, 10 mM glutamate and 2.5 mM AcCoA in a 100 µl reaction volume. The reaction was initiated by the addition of enzyme, and the mixture was incubated at 303 K for 5 min, then quenched with 100 µl of 30% trichloroacetic acid containing 50 µg of *N*-acetyl-[$^{13}C_5$] glutamate (^{13}C-NAG) as an internal standard. Precipitated protein was removed by micro-centrifugation. The supernatant (10 µl) was submitted to LC–MS (Agilent) for separation and measurement. The mobile phase consisted of 93% solvent A (1 ml trifluoroacetic acid in 1 L water) and 7% solvent B (1 ml trifluoroacetic acid in 1 L of 1:9 water/acetonitrile) and the flow rate was 0.6 ml/min. L-glutamate, NAG and ^{13}C-NAG were detected and quantified by selected ion monitoring mass spectrometry.

2.4. Crystallization

Crystals of mmNAGS/K-Arg were grown in the presence of L-arginine by the sitting drop, vapor-diffusion method. Before crystallization, the purified protein (~10 mg/ml) was incubated with 1 mM L-arginine, and 10 mM NAG for 30 min. Screening for crystallization conditions was performed using sitting drop vapor diffusion in 96-well plates (Hampton Research) at 291 K by mixing 2 µl of the protein solution with 2 µl of the reagent solution from the sparse matrix Crystal Screens 1 and 2, and Index Screen (Hampton Research). The best crystals were grown from a reservoir solution containing 100 mM sodium cacodylate trihydrate, pH 6.2, 25% polypropylene glycol P400 and 200 mM magnesium chloride. Crystal were plate-shaped and reached a maximum length of 0.4 mm in 6–7 days.

2.5. Data collection and structure determination

Crystals were transferred from the crystallization plate to a well solution supplemented with 25% glycerol and then vitrified directly by liquid nitrogen. Diffraction data were collected at beamline 22-ID equipped with a MAR300 CCD at the Advanced Photon source (APS), Argonne National Laboratory, USA. All data were processed using the HKL2000 package [9]; statistics are summarized in Table 1. The structure was solved by molecular replacement using Phaser [10,11] and subunit X of the mmNAGS/K-CoA structure (PDB 3S6G) as the search model. After several cycles of refinements with Phenix [12] and model adjustments with Coot [13], L-arginine was visible in the electron density map and built into the model. Although NAG was included in the crystallization medium, it was not visible in the crystals at any stage of the refinement. In the last stage of refinement, the translation/liberation/screw (TLS) parameters were included and refined [14]. Five TLS groups per subunit were selected in the *N*-terminal segment, *N*-terminal lobe and the *C*-terminal lobe of the AAK domain and the *N*-terminal arm and the *C*-terminal arm of NAT domain, as defined previously [5]. The final R and R_{free} were 19.9% and 26.5%, respectively. Refinement statistics for the final refined model are given in Table 1. The final refined coordinates for mmNAGS/K-Arg have been deposited in the RCSB Protein Data Bank with the accession code 4KZT. All figures were drawn using program Pymol [15].

Table 1
Data collection and refinement statistics.

Data collection	
Bound ligands	L-arginine
Space group	*C*2
Wavelength (Å)	1.0
Resolution (Å)	40–2.80 (2.85–2.80)[a]
Unit-cell parameters (Å)	a = 165.8 Å b = 110.8 Å c = 117.2 Å β = 91.0°
Measurements	312,380
Unique reflections	47,676 (1431)
Redundancy	6.6 (2.9)
Completeness (%)	90.3 (54.1)
$\langle I/\sigma(I)\rangle$	37.0 (1.5)
R_{merg}(%)[b]	8.1 (65.6)
Refinement	
Resolution range (Å)	40–2.79 (2.86–2.79)
No. of protein atoms	13244
No. of water atoms	0
No. of hetero atoms	76
Rmsd of bond lengths (Å)	0.009
Rmsd of bond angle (°)	1.4
R_{work} (%)[c]	19.6 (37.8)
R_{free} (%)[d]	26.5 (48.2)
Ramachandran plot (%)	
Favored	83.3
Allowed	13.5
Generous	2.4
Disallowed	0.9

[a] Figures in brackets apply to the highest-resolution shell.

[b] $R_{merg} = \sum_h\sum_i|I(h,i)-<I(h)>|/\sum_h\sum_i I(h,i)$, where $I(h,i)$ is the intensity of the ith observation of reflection h, and $<I(h)>$ is the average intensity of redundant measurements of reflection h.

[c] $R_{work} = \sum_h||F_{obs}|-|F_{calc}||/\sum_h|F_{obs}|$.

[d] $R_{free} = \sum_h||F_{obs}|-|F_{calc}||/\sum_h|F_{obs}|$ for 5% of the reserved reflections.

3. Results and discussion

3.1. Structure of mmNAGS/K bound with L-arginine

mmNAGS/K co-crystallized with L-arginine in space group *C*2 with unit-cell parameters $a = 165.8$ $b = 110.8$ and $c = 117.2$ Å, $\beta = 91.0°$. The NAG present in the crystallization medium was not visible in the crystal and apparently does not bind under these conditions. There were four subunits in the asymmetric unit (Fig. S1), as was the case for mmNAGS/K without L-arginine bound, which crystallized in the space group of $P2_12_12_1$. Both crystal forms have similar solvent content (52–54%) with Matthews' coefficients of 2.5–2.7 Å^3/Da [16]. However, the four subunits in the mmNAGS/K-Arg structure are very similar, with RMSD values of 0.4–0.9 Å (Fig. S2A and Table S1), in contrast to those in the NAGS/K-CoA structure which are in different conformations [5]. In the mmNAGS/K-Arg structure, the conformations of subunits related by the molecular symmetric center (subunits A and Y, and subunits B and X) are more similar than are the conformations of adjacent subunits (Subunits A and B, or subunits A and X). Relative to mmNAGS/K-CoA (PDB 3S6G), the conformation of the subunits in mmNAGS/K-Arg are more similar to subunits B and X, with RMSD of 1.42 and 1.31 Å, respectively, than to subunits A and Y, with RMSD of 1.82 and 3.22 Å, respectively (Table S1).

3.2. L-arginine binding site

L-arginine binds in a cavity in the AAK domain surrounded by the central β-sheet (strands β10, β12 and β11), helix α10, the loop connecting helix α10 and strand β12, and the short *C*-terminal segment of helix α2 (Fig. 1A). Helix α12, which is from the NAT domain and almost perpendicular to helix α13 and the β-sheet of the *N*-terminal arm of the NAT domain, is close to the L-arginine binding site. Therefore, the L-arginine binding site is located in the *C*-lobe of the AAK domain and the interface between AAK and NAT domains. The structure around this site allows most main chain oxygen atoms to orient towards the binding site so that they can hydrogen bond with L-arginine (Table S2). The side-chains of four residues, Ser225 from strand β10, Ser265 from strand β11, Lys206 from strand β9 and Glu277 from helix α10 are also involved in binding L-arginine. L-arginine binds in such a way that its C_α atom is close to the side chain of Tyr28 in helix α2, its α-carboxyl group orients towards the central β-sheet of the AAK domain and its side-chain extends towards the α10-β12 connecting loop. This

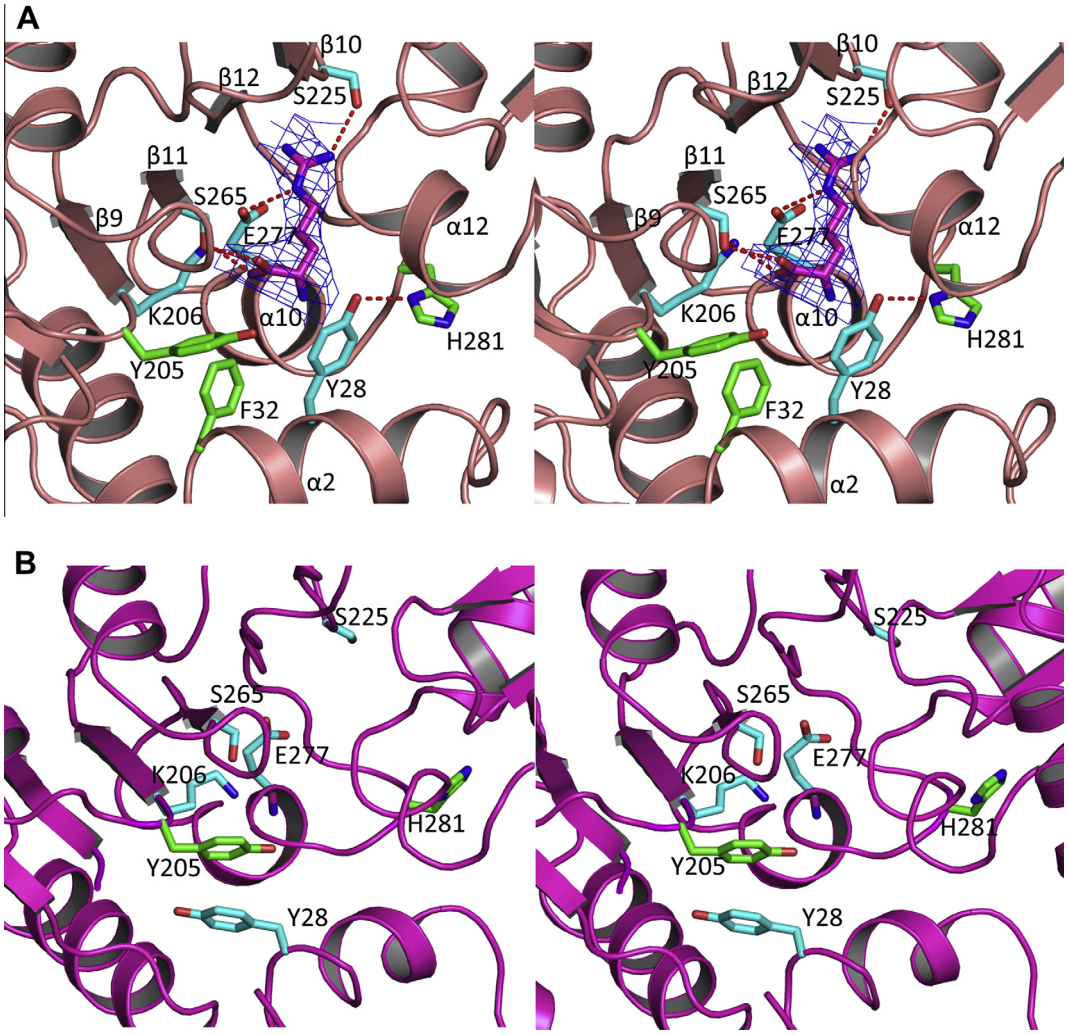

Fig. 1. Details of L-arginine binding site. (A) L-Arginine binding site (subunit A) in mmNAGS/K-Arg. Bound L-arginine is shown in pink sticks. The side chains involved in binding L-arginine are shown in light blue sticks. The side chains for other relevant residues are shown in green sticks. The electron density map ($2F_o-F_c$) around bound L-arginine (contoured at 1.0 σ) is shown as a blue cage. The potential hydrogen bonding interactions are shown in red dashed lines. (B) Arginine binding site (Subunit Y) in mmNAGS/K-CoA.

binding site is very similar to the L-arginine binding sites of NAGK enzymes from *Thermotoga maritima* (tmNAGK; PDB 2BTY) [4] and *Saccharomyces cerevisiae* (PDB 3ZZH) [6] and ngNAGS (PDB 3D2P) [17].

3.3. L-arginine induces structural changes

If we assume that the structure of subunit Y in mmNAGS/K-CoA, which has the largest conformational difference from the mmNAGS/K-Arg subunit structures, represents the active state which allows the catalytic reaction to occur, the differences between the NAGS/K-Arg structure and subunit Y in mmNAGS/K-CoA are likely to reflect the structural changes induced by L-arginine binding. To define these structural changes, subunit Y of mmNAGS/K-CoA was superimposed on subunit A of mmNAGS/K-Arg, using the core β-sheet of the AAK domain as the reference (Fig. S2B). It is immediately obvious that significant changes in the relative orientation between the AAK and NAT domains occur. Using the core β-sheet of the NAT domain to calculate the change in orientation, L-arginine binding induces an approximately 22° rotation of the NAT domain towards the AAK domain, with the linker as a hinge.

In addition to the shift in the relative orientations of the AAK and NAT domains, significant local conformational changes occur. The side chain of Tyr28 rotates approximately 180° around its C_α–C_β bond so that instead of pointing away from the L-arginine binding site it points towards it. The side chain of Phe32 moves into the L-arginine binding site to form a new hydrophobic interaction with Tyr28. In addition, its side chain oxygen hydrogen bonds

Table 2
Synthase activities of mmNAGS/K and xcNAGS/K active site mutants.

Sample	Activity (μmoles/min-mg)
mmNAGS/K	
WT	6.81 ± 0.23[a]
Y397F	Nd
S387A	4.97 ± 0.19
K356H	Nd[b]
R386K	Nd
N391Q	Nd
xcNAGS/K	
WT	44.05 ± 0.21
Y405F	Nd
S395A	39.87 ± 0.35
K364H	0.47 ± 0.15
R394K	1.66 ± 0.04
N399Q	3.11 ± 0.05

[a] Means ± standard error of means (n = 3) are shown.
[b] Nd, not detectable.

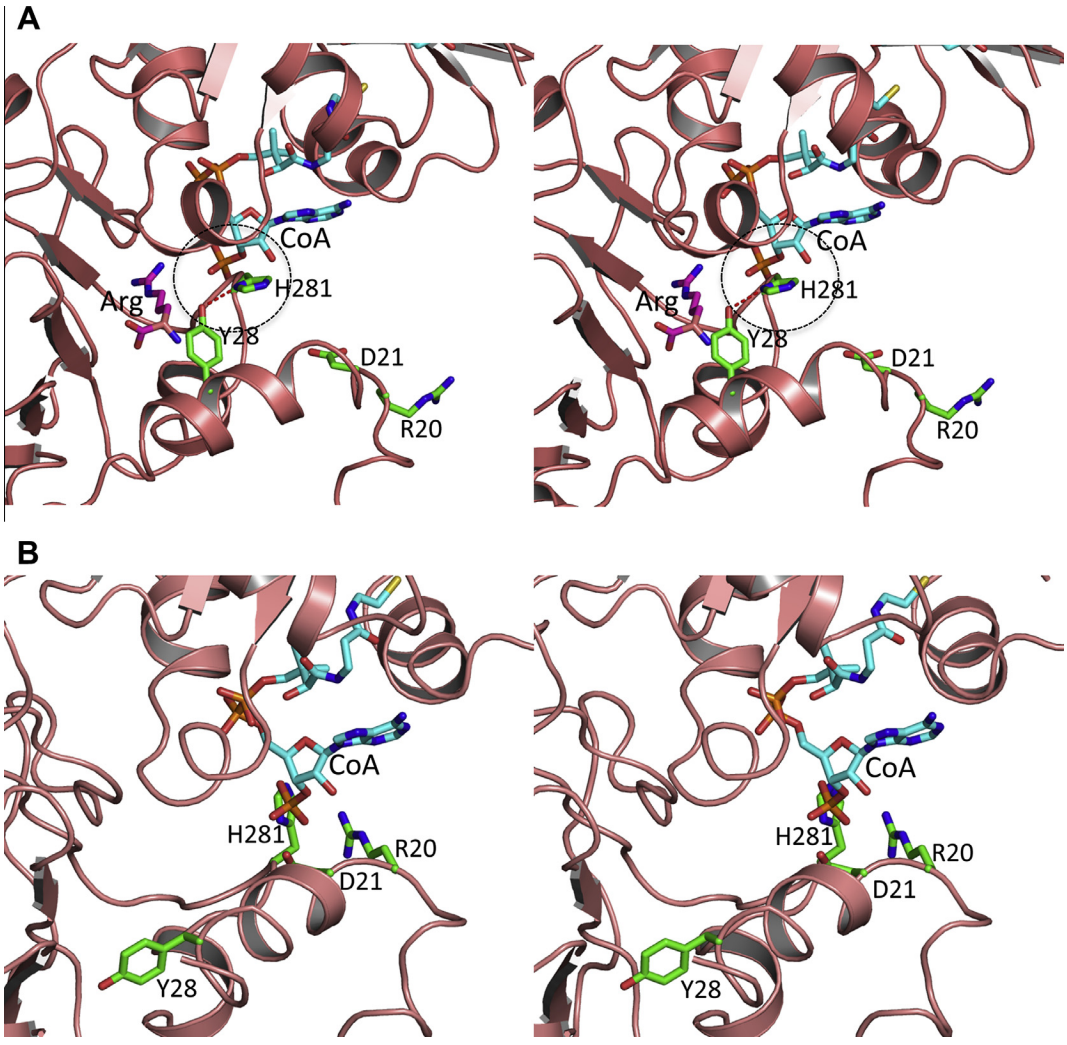

Fig. 2. Proposed L-arginine inhibition mechanism. (A) Details of interface between AAK and NAT domain in mmNAGS/K-Arg (subunit A) show the potential steric clash (shown in dashed circle) between bound CoA with the L-arginine binding loop in the mmNAGS/K-Arg structure. Bound L-arginine is shown in pink sticks. Modeled bound CoA is shown in light blue sticks. The side chains of other relevant residues are shown in green sticks. Potential hydrogen bonding interactions are shown in red dashed lines. (B) Equivalent site in the mmNAGS/K-CoA (subunit Y).

to the side chain of His281 (Fig. 1A). Formation of these interactions is accompanied by movement of the *N*-terminal helices (α1 and α2) and the L-arginine binding loop (α10-β12 loop) (Fig. S2B). In mmNAGS/K-CoA, the side chain of Tyr28 forms π−π type interactions with the side chain of Tyr205 (Fig. 1B). Movement of the side chains of residues equivalent to Tyr28 can also be observed in L-arginine-sensitive tmNAGK (Tyr15), ngNAGS (Tyr17) and yNAGK (Tyr87) [6]. Upon L-arginine binding to tmNAGK, the side chain of Tyr15 moves into interact with Arg270. In ngNAGS, the corresponding residue, Tyr17, moves into interact with Asn336. Upon L-arginine binding, Tyr87 in yNAGK moves into the L-arginine binding site to interact with Asp341, despite the fact that yNAGK has no NAGS activity.

3.4. Active site and catalytic mechanism

Even though structural comparison of the NAT domain of mmNAGS/K with other GCN5-related acetyltransferase domains including ngNAGS clearly indicated that the substrate binding sites are in the NAT domain and are located in the cleft between strands β16 and β17, the active site has not been defined experimentally. To confirm the active site and investigate the catalytic mechanism, several residues in this site were selected for biochemical studies. Tyr397 in mmNAGS/K and the equivalent residue, Tyr405, in xcNAGS/K have been proposed to function in the catalytic mechanism by donating protons to the thiol group of the leaving group, CoA (Fig. S3). The equivalent tyrosine can be identified in most GCN5-related acetyltransferases [18]. Indeed, the Y397F mutant in mmNAGS/K and the Y405F mutant in xcNAGS/K have no NAGS activity (Table 2). In contrast, mutations in the adjacent residues, Ser387 in mmNAGS/K and Ser395 in xcNAGS/K, which might potentially be alternative catalytic acids [19], reduced activity only slightly, implying that they are not critical residues in substrate binding and the catalytic reaction. Lys356, Arg386 and Asn391 in mmNAGS/K, and the equivalent residues, Lys364, Arg394 and Asn399 in xcNAGS/K, have also been proposed to be involved in binding L-glutamate [5]. The results of mutating these residues demonstrate that they indeed are critical to NAGS activity (Table 2). These results clearly demonstrate that the active site is located in the cleft between strands β16 and β17 in the NAT domain, consistent with the recent structural determination of the *N*-acetyltransferase domain of human NAGS bound with NAG [2]. In the current structure, some residual electron density was observed in this site, which was modeled as diethylene glycol.

3.5. Arginine regulatory mechanism

To investigate how the conformational changes induced by L-arginine binding affect NAGS activity, CoA and NAG were modeled into the confirmed active site by superimposing the NAT domains of ngNAGS (PDB 3B8G) and human NAGS (PDB 4K30) onto the current L-arginine liganded mmNAGS/K structure. It is immediately obvious that in this conformation the adenine group of CoA would have a steric clash with the L-arginine binding loop (Fig. 2A). In contrast, in the open conformation, as represented by subunit Y structure of mmNAGS/K-CoA, no such clash occurs; instead, after minor adjustments, the side-chains of Arg20, Asp21 and His281 may contribute to the binding of AcCoA through hydrogen bonding interactions (Fig. 2B). Therefore, the L-arginine bound mmNAGS/K structure confirms the L-arginine regulatory mechanism proposed previously [5]: binding of L-arginine induces relative domain movement between AAK and NAT domains which closes the AcCoA binding site so as to inhibit NAGS activity. This allosteric mechanism differs significantly from that of the classic bacterial NAGS, ngNAGS, even though L-arginine binds at a similar site in the AAK domain. In ngNAGS, which is a hexamer rather than a tetramer, binding of L-arginine induces large conformational changes that enlarge and shorten the hexameric ring and re-orient the NAT domains relative to the AAK domains by 109°. As a result, the different surface of the NAT interacts with AAK domains, disordering the L-glutamate binding loops and decrease NAGS activity [17].

Acknowledgments

This work was supported by Public Health Service Grants DK-DK064913 (MT). We thank Dr. David Davies for facilitating the use of the diffraction equipment in the Molecular Structure Section of the National Institutes of Health and Dr. Fred Dyda for help in data collection. High resolution data were collected at Southeast Regional Collaborative Access Team (SER-CAT) 22-ID beamline at the Advanced Photon Source, Argonne National Laboratory. Use of the Advanced Photon Source was supported by the U.S. Department of Energy, Office of Science and Office of Basic Energy Sciences, under Contract No. W-31-109-Eng-38.

Appendix A. Supplementary data

Supplementary data associated with this article can be found, in the online version, at http://dx.doi.org/10.1016/j.bbrc.2013.07.003.

References

[1] Q. Qu, H. Morizono, D. Shi, M. Tuchman, L. Caldovic, A novel bifunctional *N*-acetylglutamate synthase-kinase from Xanthomonas campestris that is closely related to mammalian *N*-acetylglutamate synthase, BMC Biochem. 8 (2007) 4.
[2] G. Zhao, Z. Jin, N.M. Allewel, M. Tuchman, D. Shi, Crystal structure of the *N*-acetyltransferase domain of human *N*-acetyl-L-glutamate synthase in complex with *N*-acetyl-L-glutamate provides insights into its catalytic and regulatory mechanisms, PLoS ONE (2013).
[3] N. Haskins, M. Panglao, Q. Qu, H. Majumdar, J. Cabrera-Luque, H. Morizono, M. Tuchman, L. Caldovic, Inversion of allosteric effect of arginine on *N*-acetylglutamate synthase, a molecular marker for evolution of tetrapods, BMC Biochem. 9 (2008) 24.
[4] S. Ramon-Maiques, M.L. Fernandez-Murga, F. Gil-Ortiz, A. Vagin, I. Fita, V. Rubio, Structural bases of feed-back control of arginine biosynthesis, revealed by the structures of two hexameric *N*-acetylglutamate kinases, from *Thermotoga maritima* and *Pseudomonas aeruginosa*, J. Mol. Biol. 356 (2006) 695–713.
[5] D. Shi, Y. Li, J. Cabrera-Luque, Z. Jin, X. Yu, G. Zhao, N. Haskins, N.M. Allewell, M. Tuchman, A novel *N*-acetylglutamate synthase architecture revealed by the crystal structure of the bifunctional enzyme from *Maricaulis maris*, PLoS ONE 6 (2011) e28825.
[6] S. de Cima, F. Gil-Ortiz, M. Crabeel, I. Fita, V. Rubio, Insight on an arginine synthesis metabolon from the tetrameric structure of yeast acetylglutamate kinase, PLoS ONE 7 (2012) e34734.
[7] D. Shi, V. Sagar, Z. Jin, X. Yu, L. Caldovic, H. Morizono, N.M. Allewell, M. Tuchman, The crystal structure of *N*-acetyl-L-glutamate synthase from *Neisseria gonorrhoeae* provides insights into mechanisms of catalysis and regulation, J. Biol. Chem. 283 (2008) 7176–7184.
[8] L. Caldovic, H. Morizono, X. Yu, M. Thompson, D. Shi, R. Gallegos, N.M. Allewell, M.H. Malamy, M. Tuchman, Identification, cloning and expression of the mouse *N*-acetylglutamate synthase gene, Biochem. J. 364 (2002) 825–831.
[9] Z. Otwinowski, W. Minor, Processing of X-ray diffraction data collected in oscillation mode, Methods Enzymol. 276 (1997) 307–326.
[10] R.J. Read, Pushing the boundaries of molecular replacement with maximum likelihood, Acta Crystallogr. D Biol. Crystallogr. 57 (2001) 1373–1382.
[11] L.C. Storoni, A.J. McCoy, R.J. Read, Likelihood-enhanced fast rotation functions, Acta Crystallogr. D Biol. Crystallogr. 60 (2004) 432–438.
[12] P.D. Adams, P.V. Afonine, G. Bunkoczi, V.B. Chen, I.W. Davis, N. Echols, J.J. Headd, L.W. Hung, G.J. Kapral, R.W. Grosse-Kunstleve, A.J. McCoy, N.W. Moriarty, R. Oeffner, R.J. Read, D.C. Richardson, J.S. Richardson, T.C. Terwilliger, P.H. Zwart, PHENIX: a comprehensive python-based system for macromolecular structure solution, Acta Crystallogr. D Biol. Crystallogr. 66 (2010) 213–221.
[13] P. Emsley, K. Cowtan, Coot: model-building tools for molecular graphics, Acta Crystallogr. D Biol. Crystallogr. 60 (2004) 2126–2132.
[14] M.D. Winn, M.N. Isupov, G.N. Murshudov, Use of TLS parameters to model anisotropic displacements in macromolecular refinement, Acta Crystallogr. D Biol. Crystallogr. 57 (2001) 122–133.
[15] L. Schrodinger, The pymol molecular System, Version 1.5.0.4 Schrödinger, LLC.
[16] B.W. Matthews, Solvent content of protein crystals, J. Mol. Biol. 33 (1968) 491–497.

[17] L. Min, Z. Jin, L. Caldovic, H. Morizono, N.M. Allewell, M. Tuchman, D. Shi, Mechanism of allosteric inhibition of *N*-acetyl-L-glutamate synthase by L-arginine, J. Biol. Chem. 284 (2009) 4873–4880.
[18] H. He, Y. Ding, M. Bartlam, F. Sun, Y. Le, X. Qin, H. Tang, R. Zhang, A. Joachimiak, J. Liu, N. Zhao, Z. Rao, Crystal structure of tabtoxin resistance protein complexed with acetyl coenzyme A reveals the mechanism for beta-lactam acetylation, J. Mol. Biol. 325 (2003) 1019–1030.
[19] G. Zhao, N.M. Allewell, M. Tuchman, D. Shi, Structure of the complex of *Neisseria gonorrhoeae N*-acetyl-L-glutamate synthase with a bound bisubstrate analog, Biochem. Biophys. Res. Commun. 430 (2013) 1253–1258.